ISSN 1001-0742
CN 11-2629/X

2012
Volume 24
Number 7

JOURNAL OF

ENVIRONMENTAL SCIENCES

ELSEVIER
Science Press

Sponsored by
Research Center for Eco-Environmental Sciences
Chinese Academy of Sciences

JOURNAL OF ENVIRONMENTAL SCIENCES

(http://www.jesc.ac.cn)

Aims and scope

Journal of Environmental Sciences is an international academic journal supervised by Research Center for Eco-Environmental Sciences, Chinese Academy of Sciences. The journal publishes original, peer-reviewed innovative research and valuable findings in environmental sciences. The types of articles published are research article, critical review, rapid communications, and special issues.

The scope of the journal embraces the treatment processes for natural groundwater, municipal, agricultural and industrial water and wastewaters; physical and chemical methods for limitation of pollutants emission into the atmospheric environment; chemical and biological and phytoremediation of contaminated soil; fate and transport of pollutants in environments; toxicological effects of terrorist chemical release on the natural environment and human health; development of environmental catalysts and materials.

For subscription to electronic edition

Elsevier is responsible for subscription of the journal. Please subscribe to the journal via http://www.elsevier.com/locate/jes.

For subscription to print edition

China: Please contact the customer service, Science Press, 16 Donghuangchenggen North Street, Beijing 100717, China. Tel: +86-10-64017032; E-mail: journal@mail.sciencep.com, or the local post office throughout China (domestic postcode: 2-580).

Outside China: Please order the journal from the Elsevier Customer Service Department at the Regional Sales Office nearest you.

Submission declaration

Submission of an article implies that the work described has not been published previously (except in the form of an abstract or as part of a published lecture or academic thesis), that it is not under consideration for publication elsewhere. The submission should be approved by all authors and tacitly or explicitly by the responsible authorities where the work was carried out. If the manuscript accepted, it will not be published elsewhere in the same form, in English or in any other language, including electronically without the written consent of the copyright-holder.

Submission declaration

Submission of the work described has not been published previously (except in the form of an abstract or as part of a published lecture or academic thesis), that it is not under consideration for publication elsewhere. The publication should be approved by all authors and tacitly or explicitly by the responsible authorities where the work was carried out. If the manuscript accepted, it will not be published elsewhere in the same form, in English or in any other language, including electronically without the written consent of the copyright-holder.

Editorial

Authors should submit manuscript online at http://www.jesc.ac.cn. In case of queries, please contact editorial office, Tel: +86-10-62920553, E-mail: jesc@263.net, jesc@rcees.ac.cn. Instruction to authors is available at http://www.jesc.ac.cn.

Copyright

ISSN 1001–0742 **Journal of Environmental Sciences** Vol. 24 No. 7 2012

CONTENTS

Serial parameter: CN 11-2629/X*1989*m*198*en*P*24*2012-7

Available online at www.sciencedirect.com
ScienceDirect
Journal of Environmental Sciences 2012, 24(7) 1305–1316
JOURNAL OF ENVIRONMENTAL SCIENCES
ISSN 1001-0742
CN 11-2629/X
www.jesc.ac.cn

Effects of WO_x modification on the activity, adsorption and redox properties of CeO_2 catalyst for NO_x reduction with ammonia

Ziran Ma[1], Duan Weng[1,*], Xiaodong Wu[1,2], Zhichun Si[3]

1. State Key Laboratory of New Ceramics & Fine Process, Department of Materials Science and Engineering, Tsinghua University, Beijing 100084, China
2. Yangtze Delta Region Institute of Tsinghua University, Zhejiang 314000, China
3. Advanced Materials Institute, Graduate School at Shenzhen, Tsinghua University, Shenzhen 518055, China

Received 30 September 2011; revised 05 December 2012; accepted 14 December 2011

Abstract

A series of WO_3/CeO_2 (WO_x/CeO_2) catalysts were synthesized by wet impregnation of ammonium metatungstate on a CeO_2 support. The resulting solid acid catalysts were characterized by X-ray diffraction (XRD), UV-Vis spectroscopy (UV-Vis), Raman spectroscopy (Raman), *in-situ* Fourier transform infrared spectroscopy (*in-situ* FT-IR) of ammonia adsorption, NH_3-TPD, H_2 temperature-programmed reduction (H_2-TPR), NH_3/NO oxidation and activity measurements for NO_x reduction by NH_3 (NH_3-SCR). The results show that polytungstate (WO_x) species are the main species of tungsten oxide on the surface of ceria. The addition of tungsten oxide enhances the Brönsted acidity of ceria catalysts remarkably and decreases the amount of surface oxygen on ceria, with strong interaction between CeO_2 and WO_x. As a result, the N_2 selectivity of NH_3 oxidation and NH_3-SCR at high temperatures (> 300°C) is enhanced. Therefore, a wide working temperature window in which NO_x conversion exceeds 80% (NO_x conversion > 80%) from 200 to 450°C, is achieved over 10 wt.% WO_x/CeO_2 catalyst. A tentative model of the NH_3-SCR reaction route on WO_x/CeO_2 catalysts is presented.

Key words: NO_x reduction; WO_x/CeO_2 catalyst; redox; NH_3 adsorption
DOI: 10.1016/S1001-0742(11)60925-X

Introduction

In light of the increasingly stringent emission standards for vehicle exhaust, interest in reducing NO_x emissions has received much attention in recent years. The most efficient technology to remove NO_x from stationary sources is the selective catalytic reduction of NO_x by ammonia (NH_3-SCR), and it is also currently the most favored technology for lean burn engine exhaust deNO_x (Busca et al., 2005). Reduction of NO_x emissions from a diesel engine requires a highly efficient catalyst which operates in a temperature range of 200–500°C and is capable of high space velocity. To meet such a requirement, a typical commercial SCR catalyst V_2O_5-$WO_3(MoO_3)/TiO_2$ (VWTi) with about 1 wt.% V_2O_5 supported on 6–10 wt.% WO_3/MoO_3 containing titania (anatase) was used first for stationary sources, and was then introduced into application in diesel vehicles (Sjövall et al., 2009; Klukowski et al., 2009; Schwidder et al., 2008). VWTi oxides have high SCR activity in the temperature range 300–500°C. Nevertheless, the high activity for oxidation of SO_2 to SO_3, rapid decrease in activity and selectivity at higher temperatures, low stability due to the phase transformation of anatase to rutile and the toxicity of the vanadia species limit their applications in diesel deNO_x (Brandenberger et al., 2008). Metal-exchanged zeolites, especially ZSM-5, have been studied extensively for removing NO_x from diesel vehicles. However, some inevitable problems with this catalyst system still remain; for example, their relatively low stability in hydrothermal aging, causing dealumination, leads to deactivation of the zeolite catalysts. Coke transformed from hydrocarbons can poison the active sites or block their access, and the regeneration of zeolite catalysts, requiring the removal of coke at high temperatures causes detrimental effects like dealumination, degradation of the zeolite and sintering of supported metals, etc. (Brandenberger et al., 2008; Grossale et al., 2008; Guisnet and Magnoux, 1997).

Extensive efforts have been made over the past decade to develop non-vanadium catalysts for deNO_x, especially CeO_2-based NH_3-SCR catalysts, which have recently been the subject of extensive development. MnO_x-CeO_2 mixed oxide showed better activity at low temperature, and the addition of niobium oxides into the catalyst was found to significantly enhance its low-temperature activity (Qi et al., 2004; Casapu et al., 2009). A strong interaction between ceria and titania was found in CeO_2-TiO_2 (Xu et al., 2009; Gao et al., 2010) and V_2O_5-CeO_2/TiO_2 catalysts (Huang et al., 2008), where a high concentration of amorphous Ce^{3+} on the surface increased the chemisorption of weakly bound oxygen species and resulted in good

* Corresponding author. E-mail: duanweng@tsinghua.edu.cn

activity. In addition, synergistic effects between CeO_2 and other species in catalysts, which could generate active oxygen species with high reducibility and increase acid sites, were also considered to promote SCR reaction in many CeO_2-containing catalysts synthesized by different methods (Gao et al., 2010; Liu et al., 2010; Si et al., 2010; Zhu et al., 2010; Adamowska et al., 2008; Reddy et al., 2003). Besides these studies, in recent years, WO_x- and CeO_2 containing catalysts have gained much attention as a result of their good activity. Li et al. (Chen et al., 2010) also reported CeO_2/WO_3-TiO_2 or CeO_2-WO_3-TiO_2 novel catalysts with high activity for NH_3-SCR of NO_x in the temperature range 200-450°C at a space velocity of 28,000 hr^{-1}. WO_3 supported on CeO_2-ZrO_2 solid solutions has been reported to show high SCR activity within a high temperature range (300–500°C) at a space velocity of 90,000 hr^{-1} in NH_3-SCR applications (Li et al., 2008). He et al. (Shan et al., 2011) reported a novel CeO_2-WO_3 mixed oxide catalyst prepared by a homogeneous precipitation method which achieved nearly 100% NO_x conversion in a wide temperature range from 250 to 425°C under an extremely high GHSV of 500,000 hr^{-1}. Their work all indicated that WO_3 crystallites can be finely dispersed over the catalyst surface to enhance the acidity of ceria catalysts, and some kind of synergetic effect between tungsten oxides and ceria promoted the SCR activity by ammonia. However, the specific synergistic effects between CeO_2 and WO_x in the mixed oxide catalysts and the corresponding SCR reaction pathways have not been discussed in depth.

In the present work, a series of WO_3/CeO_2 catalysts were prepared for the selective catalytic reduction of NO_x by NH_3. The structure of CeO_2-supported WO_x was characterized through XRD, UV-Vis and Raman spectra. By means of *in-situ* FT-IR tests of NH_3 adsorption, H_2-TPR, NH_3/NO oxidation and the activity for NO_x reduction by NH_3, the effects of tungsten oxide modification on the acidity, redox and activity of ceria catalysts were analyzed and discussed.

1 Experimental

1.1 Catalyst preparation

The catalysts were synthesized by a wet impregnation method. Corresponding amounts of ammonium paratungstate (Beijing Beihua, China), ceria power (American BASF, 310 m^2/g) and oxalic acid (Beijing Beihua, China) were used as precursors. Ammonium paratungstate, oxalic acid and deionized H_2O were mixed by the molar ratio of 1:1.5:100 to obtain a clear solution, and then the corresponding amount of CeO_2 powders was added. The mixture was stirred at 100°C until all H_2O had evaporated. After that, the resulting powders were dried at 100°C overnight and subjected to calcination at 600°C for 4 hr in static air. The catalysts were denoted as (x)WO_x/CeO_2 (XWC), where x represented the mass percentage of WO_3. The pure ceria powders were also calcined at 600°C for 4 hr in static air for use as a reference.

1.2 Activity measurement

The activity measurements for NH_3-SCR were carried out in a quartz reactor with 200 mg of catalyst (diluted to 1 mL by silica) inside. The reaction gas mixture consisted of 500 ppm NO, 500 ppm NH_3, 5% O_2 and N_2 in balance. The total flow rate of the gas mixture was 500 mL/min at a gas hourly space velocity (GHSV) of 30,000 hr^{-1}. The SCR activities of the catalysts were measured under steady-state conditions at various temperatures. The concentrations of NO_x and NH_3 were measured by a Thermo Nicolet 380 Fourier transformed infrared spectroscopy (FT-IR) detector after the NH_3-SCR reaction reached a steady state. NO_x conversion (deNO_x) was defined as follows:

$$NO_x \text{ conversion} = \frac{C_{\text{NO-in}} - C_{\text{NO-out}} - C_{\text{NO}_2\text{-out}} - 2C_{\text{N}_2\text{O-out}}}{C_{\text{NO-in}}} \times 100\% \quad (1)$$

1.3 Catalysts characterization

X-ray diffraction (XRD) experiments were performed on a Japan SHIMADZU s-7000 diffractometer employing Cu $K\alpha$ radiation (λ = 0.15418 nm) operated at 40 kV and 120 mA. The X-ray diffractograms were recorded at 0.02° intervals in the range of $20^\circ \leqslant 2\theta \leqslant 80^\circ$ with a scanning velocity of 4°/min. The crystal phases were identified using JCPDS (Joint Committee on Powder Diffraction Standards) cards, and the lattice constants and mean crystallite sizes of ceria were calculated from Cohen's method and the Williamson-Hall equation.

Brunauer-Emmett-Teller (BET) surface areas were calculated from N_2 adsorption data obtained using an F-Sorb 3400 apparatus (Gold APP Instrument) at –196°C. Before the measurement, the sample was degassed in N_2 at 200°C for 2 hr.

The Raman spectra (Raman) were obtained with a LabRAM HR 800 (HORIBA Jobin Yvon, France) spectrometer at room temperature (RT) and atmospheric pressure. An argon ion laser beam with the wavelength of 488 nm was focused on a spot 1 μm in diameter.

The UV-Vis spectra (UV-Vis) were measured in diffuse reflectance mode using a Shimadzu UV-2100S spectrometer with an internal integration sphere. A $BaSO_4$ pellet was used as a reference. The spectra were recorded at RT in the spectral range 200–800 nm.

H_2 temperature-programmed reduction (H_2-TPR) was performed in a fixed-bed reactor with the effluent gases monitored using a quadrupole mass spectrometer (MS) (Omnistar 200). Prior to the H_2-TPR experiment, the 50 mg sample was treated with 2 vol.% O_2/He with a total flow rate of 50 mL/min at 550°C for 30 min, then cooled down to RT in the same atmosphere, and subsequently flushed with 50 mL/min He for 30 min to remove the physically adsorbed molecules. Finally, the reactor temperature was raised to 900°C at a constant heating rate of 10°C/min in 5 vol.% H_2/He with a flow rate of 50 mL/min. H_2 consumption during the experiment was monitored by MS.

Ammonia temperature-programmed desorption (NH_3-TPD) experiments were carried out with a Nicolet-380 FT-IR spectroscopy detector. Before the experiment, 0.2 g catalyst was treated in 20% O_2/N_2 at 500°C for 30 min. After cooling down to RT, the sample was exposed to 1000 ppm NH_3/N_2 for 30 min and flushed with N_2 for 30 min. The experimental runs were recorded in N_2 while heating to 500°C at a heating rate of 10°C/min.

In-situ FT-IR spectra for NH_3 chemisorption were recorded using a thermo Nicolet 6700 FT-IR spectrometer. The sample was pretreated at 500°C in N_2 for 30 min. After cooling down to RT, the sample was flushed with N_2 for 30 min for background collection. Then a gas mixture containing 1000 ppm NH_3 and N_2 (100 mL/min) was passed through the sample for 1 hr. The IR spectra were collected after purging with N_2 flow for 30 min.

Ammonia oxidation experiments were carried out using a similar method to the NH_3-SCR measurement in an atmosphere of 500 ppm NH_3 and 5% O_2 in N_2. The gas concentrations were recorded after the oxidation reaction reached a steady state. Selectivity for the formation of N_2 during NH_3 oxidation (S_{N_2}, %) was defined by the following equation:

$$S_{N_2} = 1 - \frac{C_{NO_2\text{-out}} + C_{NO\text{-out}} + 2C_{N_2O\text{-out}}}{C_{NH_3\text{-in}} - C_{NH_3\text{-out}}} \times 100\% \qquad (2)$$

NO oxidation experiments were carried out using a method similar to the NH_3-SCR measurement, with 500 ppm NO and 5% O_2 in N_2.

2 Results

2.1 SCR activity

The NH_3-SCR performance of WOx/CeO_2 catalysts was measured as a function of temperature (Fig. 1a). Pure CeO_2 catalyst shows rather poor SCR activity over the whole temperature range. The SCR activities of the WO_3-modified catalysts are clearly promoted. Among the catalysts investigated, 10WC catalyst shows the highest SCR activity, obtaining over 80% NOx conversion over a wide temperature interval of 200–450°C, which is comparable to the performance of commercial V_2O_5/WO_3-TiO_2 catalyst. The N_2 selectivity of the catalysts follows the order 20WC > 10WC > 5WC > CeO_2, indicating that the modification with tungsten oxide could inhibit the formation of N_2O and NO_2 during the SCR process. The amount of NO_2, which is mainly the product of ammonia oxidation and NO oxidation, decreases with increasing tungsten oxide loading. No N_2O is observed over the WOx-modified catalysts, while considerable N_2O is generated over the CeO_2 catalyst. All these results indicate that a synergistic effect on the NH_3-SCR reaction exists between the CeO_2 support and WOx.

2.2 XRD

Figure 2 shows the XRD patterns of the catalysts with different WO_3 loading. The symmetrical peaks of all samples are consistent with the characteristic peaks of fluorite-like ceria. No obvious peaks of tungsten oxides are observed, indicating that tungsten oxides are finely dispersed on the surface of ceria. According to the variations in the average crystallite size of ceria as shown in Table 1, the WO_3 addition seems to inhibit the sintering of CeO_2. However, the blocking effect of the CeO_2 support pores by the impregnated tungsten oxide accounts for the reduced surface area of the modified catalysts.

The lattice constant of ceria was also calculated according to the Williamson-Hall equation and the results are summarized in Table 1. Generally, the lattice constant of ceria is associated with the ratio of Ce^{4+}/Ce^{3+} and possible incorporation of W^{n+} into the ceria lattice. Considering the smaller ionic radii of W^{6+} (0.060 nm) and W^{5+} (0.062 nm) compared to those of Ce^{4+} (0.087 nm) and Ce^{3+} ions (0.110 nm), the incorporation of W^{n+} cations into the CeO_2 lattice may result in shrinkage of the CeO_2 lattice.

Table 1 Structural and textural properties of the catalysts

Sample	BET surface area (m^2/g)	Crystallite size of CeO_2 (nm)	Lattice constant of CeO_2 (nm)
CeO_2	117	13.3	0.5415
5WC	92	10.8	0.5407
10WC	56	13.4	0.5406
20WC	53	10.4	0.5405

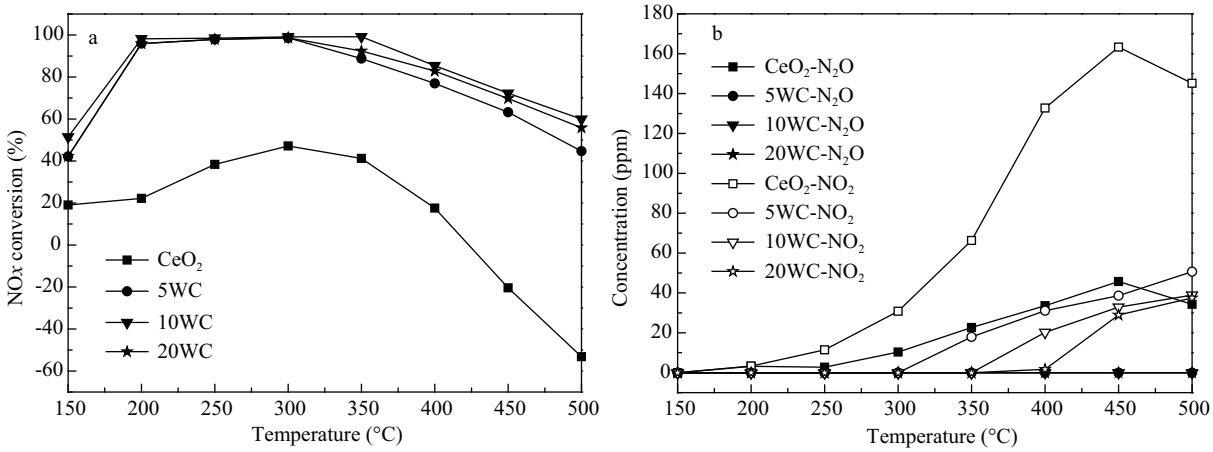

Fig. 1 SCR activity of CeO_2 and WOx/CeO_2 catalysts. (a) NOx conversion; (b) NO_2 and N_2O outlet concentration. Reaction conditions: [NO] = [NH_3] = 500 ppm, [O_2] = 5%, N_2 in balance, GHSV = 30,000 hr^{-1}. 5WC, 10WC, 20WC mean the mass percentages of WO_3 are 5%, 10%, 20%, respectively.

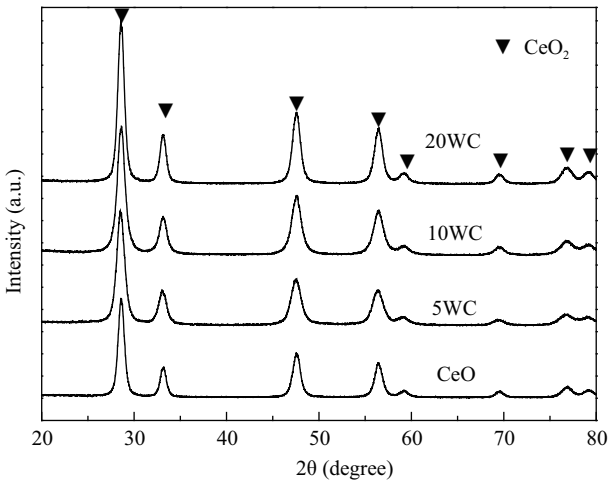

Fig. 2 XRD patterns of the catalysts.

Alternatively, the shrinkage of the ceria lattice could also be due to the decreased amount of Ce^{3+} ions caused by the interaction with tungsten oxide.

2.3 UV-Vis spectra

Figure 3 shows the UV-vis spectra of the catalysts. Ceria shows an absorption edge corresponding to the O_{2p}-Ce_{4f} transition with a band gap of 2.9 eV (Cormal et al., 2004; Tsunekawa et al., 2000). All the tungsten-containing catalysts show an absorption edge between 405 and 456 nm, with a band gap of 3.0, 2.8 and 2.5 eV for 5WC, 10WC and 20WC, respectively, which may correspond to the harmonics and combination absorption edges of the ligand-to-metal charge transfer (O_{2p}-W_{5d}-O_{2p}) of WOx species and O_{2p}-Ce_{4f} charge transfer of CeO_2. The absorption may be ascribed to defects resulting from a partial dissolution occurring at the interface of the two oxide phases. 5WC shows the lowest wavelength of the absorption edge at 405 nm. The blue shift of the absorption edge compared to CeO_2, with a band gap of 3.0 eV in 5WC, mainly results from the decrease of the Ce^{3+}/Ce^{4+} ratio in the catalyst (Tsunekawa et al., 2000). The lattice relaxation of ceria by tungsten modification may induce the oxidation of Ce^{3+} to Ce^{4+}, decreasing the charge transfer gap between the O_{2p} and Ce_{4f} bands. Such an absorption edge shift depends on the extent of WO_3 loading, which is consistent with the literature (Singh and Singh, 2011; Yagoubi and Hogarth, 1993). The gradual increase in the surface density of tungsten oxide increases the concentrations of octahedral [WO_6] and tetragonal [WO_4] units, which causes the creation of a large number of donor centers which can accept electrons from O_{2p} and then donate them to Ce_{4f}. As a result, the impurity band becomes more extended into the main band gap. This development shifts the absorption edge towards lower energies, leading to a significant shrinkage of the band gap. This can be attributed to the strong electron interaction between CeO_2 and WOx species. Moreover, the increased size of WOx domains, which cannot be detected in XRD patterns, can also result in continuously decreasing E_g values (Lin et al., 2009; Barton et al., 1999; Onfroy et al., 2005).

2.4 Raman spectra

Figure 4 shows the Raman spectra of the catalysts. In contrast to the XRD patterns that give information related mainly to the cation sublattice, the Raman spectrum is dominated by the oxygen lattice vibration of CeO_2 and the surface structure of WOx on ceria (Wachs et al., 2006; Wang et al., 2007; Bigey et al., 2001). The band around 460 cm^{-1} is ascribed to the F_{2g} Raman-active mode of the cubic fluorite structure (Wang et al., 2007; Mineshige et al., 2000; Vidal et al., 2000). This band shifts from 455 cm^{-1} for CeO_2 to 461, 463 and then back to 460 cm^{-1} for 5WC, 10WC and 20WC, respectively. These shifts of peaks indicate a similar trend of variation in the crystallite size of ceria, which matches well with the XRD results in Table 1 (Reddy et al., 2002, 2003). It is known that the intensity of Raman band depends on several factors, including the grain size and morphology.

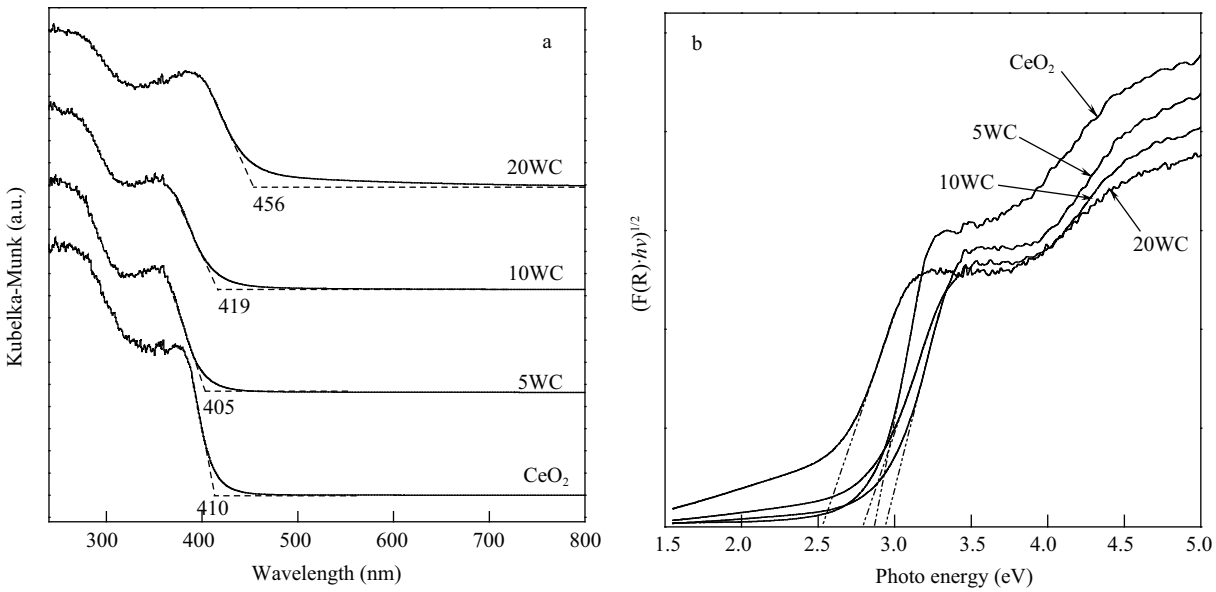

Fig. 3 UV-Vis spectra of WOx/CeO_2 catalysts. (a) plotted as the Kubelka-Munk function vs. wavelength; (b) plotted as the $(F(R)h\nu)^{1/2}$ function vs. photon energy.

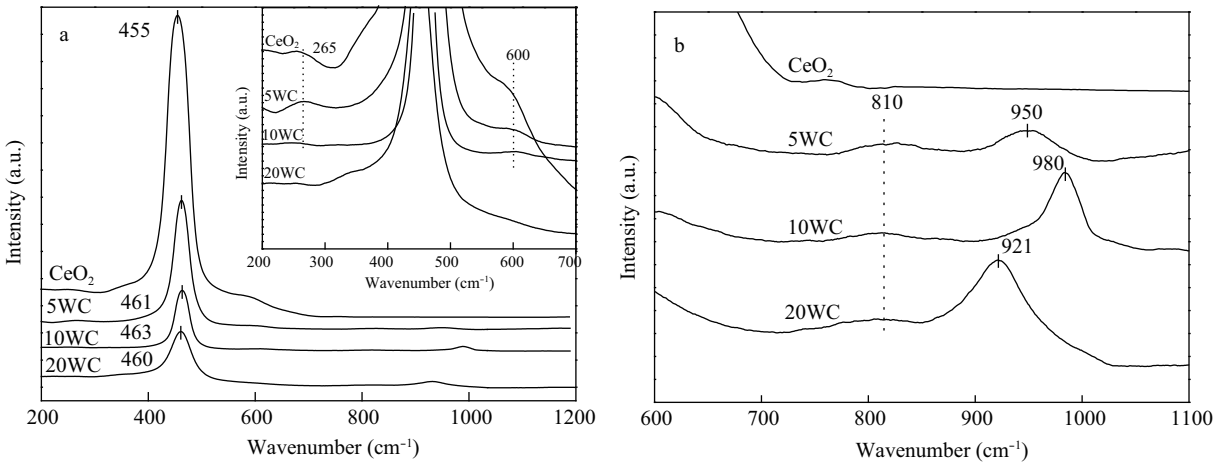

Fig. 4 Raman spectra of the WOx/CeO_2 catalysts in the wavenumber range of (a) 200–1200 and (b) 600–1100 cm^{-1}.

However, all these F_{2g} bands are weakened and become less symmetrical with the increase of WOx content, as seen in Fig. 4a. Considering the increasing size of ceria crystallites as reflected by the XRD results, it is reasonable to suggest that the surface content of ceria decreases as a consequence of WOx coverage and a stronger interaction between CeO_2 and surface tungsten oxide species. The bands at 265 and 600 cm^{-1} indicate the presence of some defects in CeO_2, which could lead to a relaxation of selection rules. In particular, these bands have been linked to oxygen vacancies in the CeO_2 lattice (Wang et al., 2007; Mineshige et al., 2000; Vidal et al., 2000) which disappear when the WO_3 loading exceeds 5%.

Raman spectroscopy gives additional structural information about tungsten species in catalysts. Tungsten-containing catalysts exhibit a band at 810 cm^{-1} assigned to W–O stretching modes (A_{1g}) (Bigey et al., 2001; Mamede et al., 2004; Huang et al., 2007; Cortés-Jácome et al., 2007), which is a typical characteristic of polytungstate species possessing [WO_5/WO_6] coordination (Wachs et al., 2006; Bigey et al., 2001; Mamede et al., 2004; Huang et al., 2007). The bands at 921–1000 cm^{-1} are ascribed to terminal W=O groups, which correspond to [WO_4] coordination in polytungstate species (Wachs et al., 2006; Bigey et al., 2001; Mamede et al., 2004; Huang et al., 2007). No bands of nano-crystallite WO_3 particles are observed, as indicated by the absence of bands at 714 cm^{-1} assigned to W–O stretching modes (E_g) and 271 cm^{-1} assigned to the W–O–W bending mode (F_{2g}) (Lin et al., 2009; Wachs et al., 2006; Bigey et al., 2001; Mamede et al., 2004). This indicates a high dispersion of WOx on these catalysts in the form of surface polytungstate species, which correlates well with the XRD and UV-Vis results. Compared with 5WC, the band assigned to the W=O vibration for the 10WC sample shifts from 950 to 980 cm^{-1}. This W=O band becomes larger with increasing surface density of tungsten oxide, which is related to polymerization of the surface WOx species (Wachs et al., 2006; Kim et al., 2007). However, the W=O vibration band shifts to lower wavenumber at 921 cm^{-1} for 20WC, implying a strong interaction between ceria and tungsten in parallel with the decrease of surface CeO_2 content, which is found to be similar to a published report that the typical band of a W=O vibration affected by Ce–O bonds is located near 920 cm^{-1} (Mamede et al., 2007).

2.5 NH_3 adsorption

NH_3-derived species on the WOx-CeO_2 catalysts were investigated by FT-IR spectroscopy, and the results are shown in Fig. 5. Bands at 1437, 1663, 2791, 3000 and 3196 cm^{-1}, which are only observed on the tungsten-containing catalysts, are assigned to NH_4^+ species on Brönsted acid sites (Zhu et al., 2010; Ramis et al., 1999; Vargas et al., 2007). These bands of NH_4^+ species increase with increasing WOx loading, indicating that Brönsted acid sites mainly arise from polymerized WOx. Bands at 1061–1241 and 3393 cm^{-1} are attributed to NH_3 coordinated to Lewis acid sites (Mamede et al., 2004; Ramis et al., 1999; Vargas et al., 2007) which are found on both ceria and the WOx-modified ceria, and their intensity decreased with increased WOx loading. Bands at 1554, 1300 and 1136 $cm^{-1}$are assigned to the NH_2 shear vibration, swing vibration and rocking vibration, respectively (Zhu et al., 2010; Ramis et al., 1999). These results clearly indicate that Lewis acid sites are much more prevalent on the CeO_2 catalyst, while WOx-CeO_2 catalysts mainly possess Brönsted acidity. WO_3 has been reported as an important additive that increases the amount and strength of Brönsted acid sites for V_2O_5-WO_3/TiO_2 catalysts (Sjövall et al., 2009; Klukowski et al., 2009; Schwidder et al., 2008). The negative band at 1003 cm^{-1} is typical for the fundamental overtone of the W=O stretching mode of surface polytungstate species (Onfroy et al., 2005; Vargas et al., 2007). Besides these, large amounts of NH_2 are present on pure ceria due to the de-protonation of ammonia coordinated on Lewis acid sites by active surface oxygen on ceria. No bands of NH_2 are observed when the loading amount of tungsten oxide exceeds 10%, suggesting that ammonia oxidation may be inhibited by tungsten oxide modification.

NH_3-TPD experiments were performed to evaluate the acidity of the catalysts. The low-temperature (100–200°C) peaks around 130°C are ascribed to the desorption of physically weakly-adsorbed ammonia, which is prone to desorb at temperatures above 200°C. Therefore, this kind of adsorbed ammonia cannot be used to evaluate the acidity of the catalysts. The high-temperature peaks are ascribed

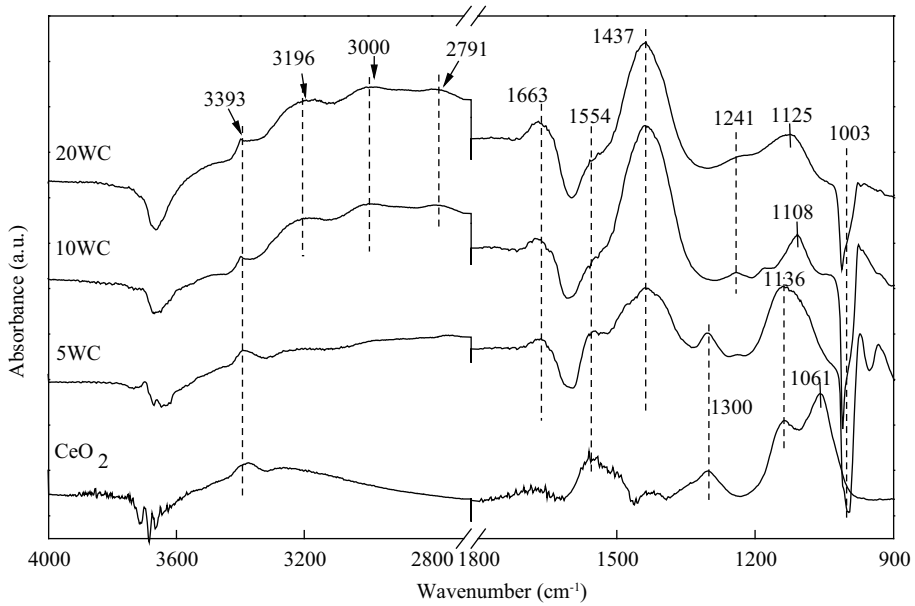

Fig. 5 FT-IR spectra of ammonia derived species on catalysts at room temperature.

to chemisorbed ammonia, which can reflect information on acid sites on catalysts. As shown in Table 2, compared with CeO_2, the acid site density (total number of acid sites per unit BET area) of 5WC decreased from 0.88 to 0.70 μmol/m^2. This is ascribed to the blocking of coordinately unsaturated Ce^{4+}(Lewis acid sites) by the supported tungsten oxides (Onfroy et al., 2005; Cortés-Jácome et al., 2007), which can explain the decreasing intensity of bands attributed to Lewis acid sites. For the WOx-containing catalysts, with the increase of the tungsten content, more ammonia is desorbed, representing the increase of acidity of the catalysts. Combined with the results above, stronger acidity is mainly brought about by the greater number of Brönsted acid sites.

Table 2 Acidity of catalysts derived from NH_3-TPD experiment

Catalyst	WO_3 loading (wt.%)	Acidity	
		Acid site density (μmol/m^2)	T_m (°C)
CeO_2	0	0.88	192
5WC	5	0.70	227
10WC	10	0.80	251
20WC	20	0.98	235

2.6 *In-situ* DRIFTS of NH_3 adsorption

Figure 6 shows DRIFT spectra of NH_3-derived species on CeO_2 and 10WC catalysts by N_2 purging at various temperatures. In Fig. 6a, bands at 1560, 1310 and 1138 cm^{-1} are ascribed to NH_2 (scissoring, wagging and rocking modes respectively) arising from ammonia oxidation on the surface of ceria. The band at 1067 cm^{-1} is contributed to NH_3 (σ_{as}) on Lewis acid sites (Zhu et al., 2010; Mamede et al., 2004; Ramis et al., 1995). The weak bands at 1435 and 1666 cm^{-1} are attributed to NH_4^+ (σ_s) and NH_4^+ (σ_{as}) on Brönsted acid sites (Mamede et al., 2004; Ramis et al., 1995). As indicated by the bands of NH_3-derived species, N_2 purging at 300°C causes the overall desorption of NH_3 and NH_4^+ species on ceria.

Figure 6b shows the spectra of NH_3-derived species on the 10WC catalyst. Both coordinated ammonia ($NH_3(\sigma_s)$: 1254, 1178 and 1117 cm^{-1}) and ammonium ions (NH_4^+ (σ_s): 1417–1436 cm^{-1}; NH_4^+ (σ_{as}): 1672 cm^{-1}) are observed on the catalyst. Two bands for coordinated ammonia indicated that ammonia is coordinated on two different Lewis acid sites, i.e., Ce^{n+} and W^{n+}. Compared with CeO_2 in Fig. 6a, tungsten modification leads to the formation of more ammonium ions involving W-OH centers, as indicated by the intense band at 1436 cm^{-1}. In addition, no protonation of NH_3 (NH_2) is observed, indicating that ammonia oxidation on ceria is effectively inhibited by WOx modification. The adsorbed NH_3 species could even exist stably at 400°C after N_2 purging, indicating that tungsten oxide modification can enhance the stability of adsorbed NH_3 on CeO_2, which, to some extent, favors the SCR reaction at high temperatures.

2.7 H_2-TPR

Figure 7 shows the H_2-TPR profiles of the catalysts. Pure ceria presents a sharp reduction peak at 320°C and a broad peak at about 770°C. The low-temperature peak is associated with the reduction of surface active oxygen, and the high-temperature one is attributed to the reduction of bulk oxygen in ceria (Zhu et al., 2010). All WO_3/CeO_2 catalysts show two defined peaks in the temperature range of 500–600°C and 700–800°C. Bulk WO_3 can be reduced by H_2 via multiple steps: $WO_3 \rightarrow WO_{2.9} \rightarrow WO_2 \rightarrow W$, with three reduction peaks at 430°C ($WO_3 \rightarrow WO_{2.9}$), 630°C ($WO_{2.9} \rightarrow WO_2$) and 730°C ($WO_2 \rightarrow W$) (Barton et al., 1999; Santiesteban et al., 1999). Accordingly, the peak at 500–585°C is assigned to the WO_3 to WO_2 reduction process and the reduction of some surface ceria. The broad overlapping peak centered at 730°C is attributed to the reduction of WO_2 to W as well as bulk CeO_2. Clearly, the reduction peak of surface CeO_2 decreases in intensity and shifts to higher temperatures from 320 to 500°C at the very start of the addition of tungsten oxide,

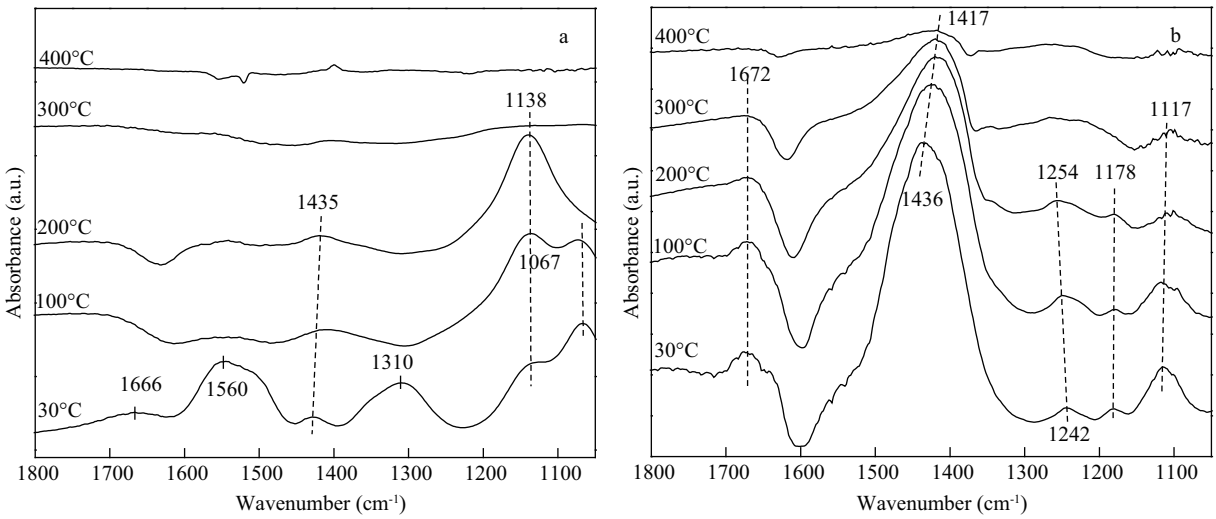

Fig. 6 DRIFT spectra of NH_3 derived species over CeO_2 (a) and 10WC (b) catalyst arising from contact of NH_3 at different temperatures.

indicating that the active surface oxygen on the CeO_2 surface is diminished by WOx modification to a large extent. The first reduction peak of the WOx-containing catalysts shifts to high temperatures with increased WOx loading, revealing a strong interaction between CeO_2 and WOx species.

Table 3 lists the H_2 reduction characteristics of the samples, of which the last column is the theoretical consumption of H_2 due to reduction of WO_3 to WO_2. The reduction of WO_3 to WO_2 is always considered to be sensitive to the size of WOx domains: the reduction becomes easier with the increased size of WOx domains on WOx/ZrO_2, WOx/SiO_2 and WOx/Al_2O_3, with the reduction of WO_3 to WO_2 at about 630°C (Barton et al., 1999; Santiesteban et al., 1999). In this work, the reduction peak ranged from 500–585°C for all WOx/CeO_2 catalysts, which is lower than the above results. The initial reduction temperature of these dispersed WOx species is determined by the strength of the W–O bonds that contain oxygen shared with the support (Vargas et al., 2007). It should be noted that unlike WOx loaded on irreducible supports, the active oxygen from W–O–Ce domains is easily reduced by H_2 due to the promotion effects of CeO_2 on W^{6+} reduction in WOx/CeO_2 catalysts. Therefore, the lower reduction peak in WOx/CeO_2 catalysts can be considered as a reduction peak of the bridging oxygen from W–O–W and W–O–Ce domains. For example, more H_2 (0.305 mmol/g) is consumed at 500°C for the low-WOx-loading sample (5WC) than the theoretical H_2 consumption for reduction of WO_3 to WO_2 (0.216 mmol/g), demonstrating the above assumption. All these results show that WOx modification increases the onset temperature of WOx/CeO_2 catalysts

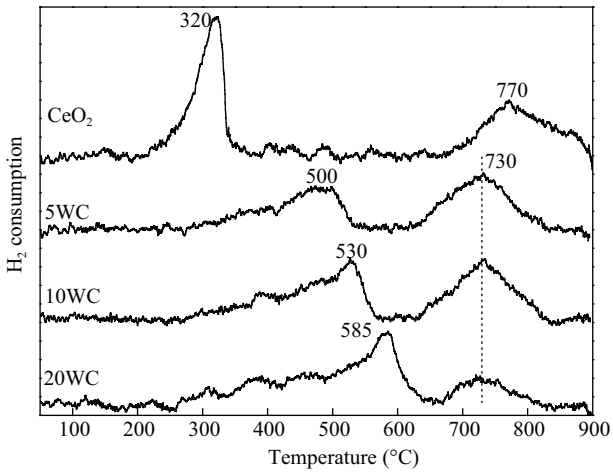

Fig. 7 H_2-TPR profiles of WOx/CeO_2 catalysts.

during H_2-TPR, while more available bridging oxygens are generated in W–O–W and W-O-Ce domains. Therefore, the reduction peak of WO_3 to WO_2 shifts to higher temperatures and the H_2 consumption of this process increases.

2.8 NH_3 oxidation and NO oxidation

Generally, ammonia oxidation and ammonia consumption by NO reduction proceed in parallel on acid sites of catalysts during the SCR reaction. It is widely accepted that at low temperatures the reaction between ammonia and NO is dominant, whereas at high temperatures oxygen becomes a more powerful oxidant than NO for ammonia oxidation (Liu et al., 2006). It is clear in Fig. 8a that the NH_3 oxidation activity of the ceria catalyst is lowered by the addition of tungsten oxide. Among the catalysts

Table 3 Redox properties of the catalysts derived from H_2-TPR results

Sample	Low-temperature peak		High-temperature peak		Theoretical H_2 consumption: reduction of WO_3 to WO_2 (mmol/g)
	Temperature (°C)	H_2 consumption (mmol/g)	Temperature (°C)	H_2 consumption (mmol/g)	
CeO_2	320	0.39	770	0.62	–
5WC	500	0.31	730	0.31	0.22
10WC	530	0.42	733	0.35	0.43
20WC	585	0.59	727	0.14	0.86

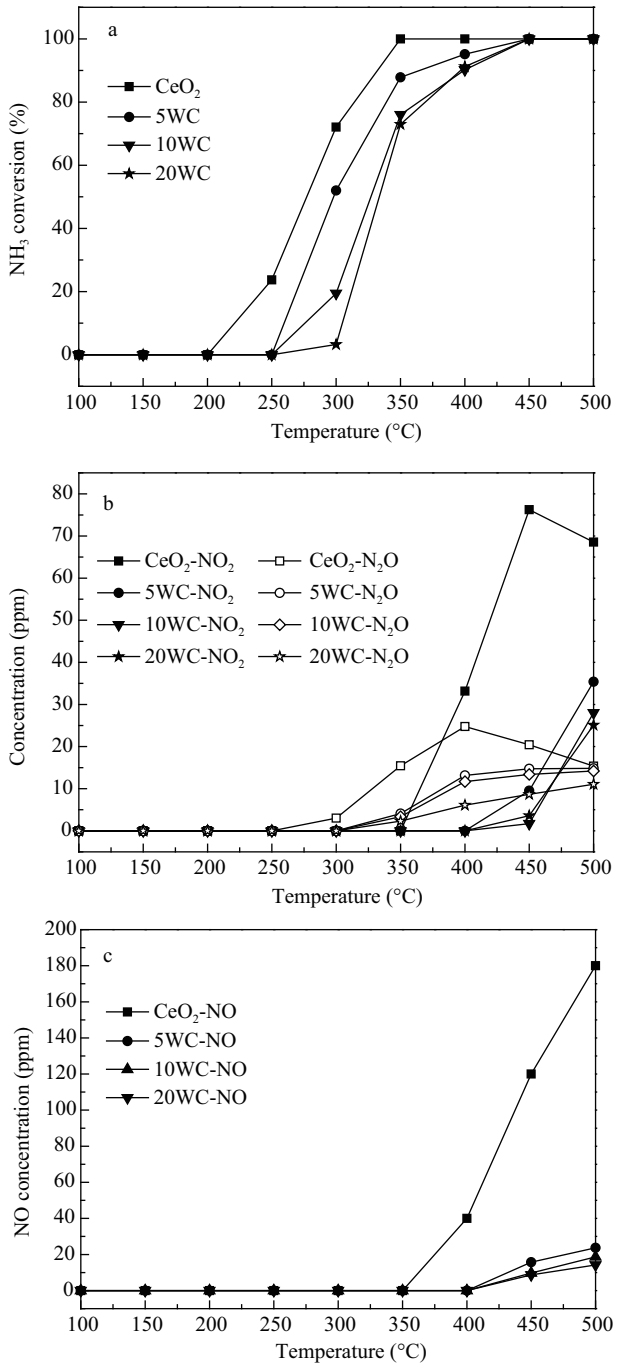

Fig. 8 NH_3 oxidation profiles of WOx/CeO_2 catalysts. (a) NH_3 conversion; (b) NO_2 and N_2O outlet concentrations; (c) NO outlet concentration.

investigated, 20WC has the lowest ammonia oxidation activity, which correlates well with the highest N_2 selectivity at high temperatures. The lower activity of ammonia oxidation for WOx/CeO_2 catalysts ensures the availability of ammonia in the SCR process at high temperatures. In Fig. 8b and c, it can be seen that ammonia could hardly be oxidized to NO, NO_2 and N_2O on all the WOx-modified catalysts, while large amounts of over-oxidized products including NO, NO_2 and N_2O are formed on ceria. The higher selectivity for WOx/CeO_2 catalysts in ammonia oxidation decreases the amount of unexpected outlet by-products.

Figure 9 shows the NO_2 concentration profiles during the NO-TPO process. NO_2 generation over ceria starts

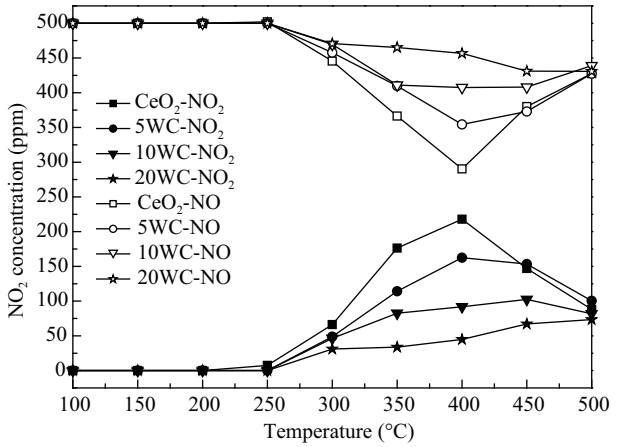

Fig. 9 NO_2 and NO outlet concentration of WOx/CeO_2 catalysts in the NO oxidation experiment.

at 250°C and reaches a maximum (250 ppm) at about 400°C due to the strong oxidation of NO. With increasing tungsten oxide loading, the oxidation of NO is gradually inhibited. The amount of NO_2 derived from NO oxidation decreases significantly with tungsten oxide modification, which can be considered to be the reason for the high N_2 selectivity obtained with the W-containing catalysts in the SCR reaction.

3 Discussion

3.1 Structure of WOx/CeO_2 catalysts

According to the WO_3 loading, the apparent surface densities of WOx are in range of 1.4–9.8W atoms/nm^2 for the WOx/CeO_2 catalysts synthesized by the impregnation method, regardless of the water used for impregnation and calcination temperatures, due to the similar BET surface area of catalysts. Some researchers found that a definite crystalline tungsten compound $Ce_2(WO_4)_3$ is preferentially formed when the surface density of W exceeds 10.8 atoms/nm^2 in WOx/CeO_2 catalysts (Mamede et al., 2004). In the present work, the formation of neither crystalline WO_3 nor the tungsten compound $Ce_2(WO_4)_3$ was detected by XRD; however, the results of UV-Vis and Raman imply the strong interaction of CeO_2 and WOx on the WC catalysts. For the given loading amount of WO_3, a stronger W-Ce interaction is created, along with more bridging oxygen in the W-Ce interface accompanied by the oxidation of Ce^{3+} to Ce^{4+}.

It has been reported that if the surface coverage of WOx on supports like ZrO_2 and Al_2O_3 is lower than a monolayer, the dominant WOx species are monomeric or polymeric tetrahedrally coordinated tungsten oxide. Tetrahedral WOx species transform to octahedrally coordinated WOx when the monotungstate polymerizes to polytungstate species. With a further increase in the tungsten surface density, WO_3 nano-particles or even bulk WO_3 may form via the polymerization of surface WOx species (Onfroy et al., 2005; Kim et al., 37; Gregorio and Keller, 2004). The XRD, UV-Vis and Raman results suggest that only highly dispersed polytungstate species formed on the WC catalysts, and no crystalline WO_3 was detected.

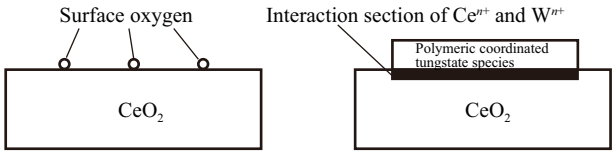

Fig. 10 Scheme of the structure evolution of CeO_2 to WOx/CeO_2.

Figure 10 shows a scheme for the structural evolution of CeO_2 to WOx-containing catalysts. WOx coverage reduces the amount of surface active oxygen, and at the same time the stronger electron interaction between $Ce^{n+}$and W^{n+} reduces the amount of oxygen vacancies and Ce^{3+}. The surface WOx polytungstate species, composed of polymeric octahedral [WO_5/WO_6] species connected by W–O bonds and tetrahedral [WO_4] species connected by W–O and W=O bonds, are highly dispersed on the catalyst surface. These highly dispersed WOx species could increase the amount of active sites on the catalyst surface for reactant adsorption and reaction.

3.2 Acidity properties

In the NH_3 adsorption experiment, both Lewis and Brönsted acid sites were observed on the WOx-CeO_2 catalysts. The acidity of catalysts increased with WOx loading, and reached the maximal acidity for the 20WC catalyst. According to the literature reports (Onfroy et al., 2005; Gregorio and Keller, 2004; Martin et al., 1998), the Lewis acid sites on WOx/CeO_2 arise from the electronically deficient unsaturated Ce^{n+} cations and W^{n+} cations in the CeO_2 and dispersed octahedral polymeric [WO_6] species. The Brönsted acid sites arise from the partially hydrated tungsten species, like the hydration of bridging Ce-O-W and W–O–W in octahedral polymeric [WO_6] species and terminal W=O in tetrahedral [WO_4] species. The acid sites on WOx-CeO_2 catalysts are able to undergo a facile transformation from Lewis to Brönsted acid sites when WOx species interact with NH_3 or H_2O (Reactions (3) and (4)). The initial decrease in Lewis acid sites on 5WC compared with CeO_2 may arise from the blocking of coordinatively unsaturated Ce^{n+}(Lewis acid sites) by the supported tungsten oxide. With further increase in the WOx loading, the formation of octahedral polymeric [WO_6] domains contributes to the increase in the amounts of both Lewis and Brönsted acid sites.

$$W{=}O + H_2O \longleftrightarrow W{-}OH + OH^- \quad (3)$$

$$W{=}O + NH_3 \longleftrightarrow W{-}OH + NH_2 \quad (4)$$

Figure 11 shows the relationship between the total acidity of the catalyst and the WOx surface density. The acidity of the catalyst was calculated from the ammonia desorption per unit BET surface of catalyst in the NH_3-TPD experiment. The (Lewis and Brönsted) acidity of the catalyst behaves as a function of the WOx surface density. According to the previous reports (Wachs et al., 2006; Kim et al., 2007), below monolayer coverage of WOx on WOx/ZrO_2 model catalysts, the surface acidity of the catalyst is mainly brought about by the polymerized WO_x species, and increases linearly with the surface density of tungsten oxide. Basically, our results demonstrate that 20 wt.% WOx content (9.8 W atoms/nm^2) does not exceed the upper limitation of monolayer surface coverage of WOx on the CeO_2 support.

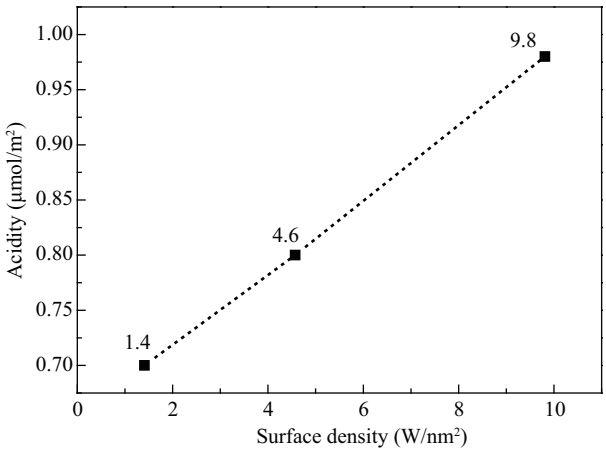

Fig. 11 The trend of the catalyst acidity as a function of tungsten oxide surface density.

3.3 Redox properties

It is seen from the H_2-TPR results that the amount of surface active oxygen on CeO_2 is reduced by WOx addition. CeO_2 is considered to possess good OSC ability. The oxygen storage capacity is tightly related to the oxygen transfer process from bulk ceria to the surface in which oxygen vacancies play an important role (Vidal et al., 2000; Reddy et al., 2002, 2003; Schulz et al., 2003). The oxygen vacancies are formed through the process as Eq. (5):

$$2Ce^{4+} \longleftrightarrow 2Ce^{3+} + \text{Vacancy } O^{2+} + O^* \quad (5)$$

According to the results of XRD, UV-Vis and Raman measurements, the impregnation of WOx on the ceria surface causes a higher degree of ceria crystallization, a lower amount of Ce^{3+} and a lower amount of oxygen vacancies in ceria, which can be ascribed to the electron-withdrawing nature of W^{6+} atoms in polytungstates. In this way, the special electron interaction between ceria and tungsten oxides causes an electron transfer from Ce^{n+} to W^{n+}, stabilizing the ceria in a relatively high valence state, which leads to a decrease in Ce^{3+} and oxygen vacancies. The decreased amount of oxygen vacancies results in the inhibition of oxygen transfer from the bulk CeO_2 phase to the surface, and this thereby would decrease the reducibility of the catalysts.

3.4 Catalytic behavior

Overall, the N_2 selectivity and NH_3-SCR activity of catalysts are controlled by the redox properties and acidity of catalysts. The reduced redox properties of ceria due to tungsten oxide modification leads to smaller production of NO_2 and NO in the NH_3 oxidation experiment and NO_2 in the NO oxidation experiment. The enhanced Brönsted acidity of ceria caused by tungsten modification results in stronger ammonia adsorption on acid sites, and the adsorbed ammonia is more stable at high temperatures. Therefore, the activity and selectivity of WOx-CeO_2 cat-

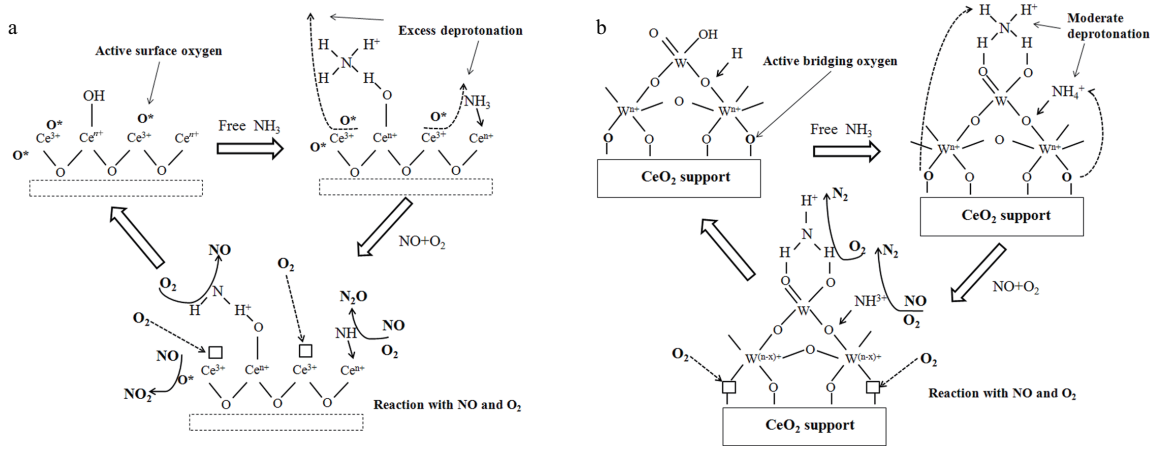

Fig. 12 Tentative models for the NH_3-SCR reaction route on CeO_2 (a) and 10WC (b) catalysts.

alysts for the NH_3-SCR reaction increase with the loading amount of WOx. NH_3 adsorbed on acid sites tends to form amide species as a result of the de-protonation of NH_3 and NH_4^+. On WOx/CeO_2 catalysts, the NH_3-SCR reaction proceeds between adsorbed amide species and gaseous nitric oxide, in which NH_2 and NH_3^+ act as important intermediates in SCR and ammonia oxidation reactions (Busca et al., 1998; Liu et al., 2006; Ramis et al., 1990; Dumesic et al., 1996). Moderate oxidation of ammonia to NH_2 species is an important step in the activation reaction, and then gaseous NO reacts with activated NH_2 to give nitrogen and water. Excessive oxidation of ammonia may generate NH or even N and subsequently N_2O and NO, leading to decreases in both SCR activity and N_2 selectivity.

The reduction of Ce^{4+} to Ce^{3+} can release active oxygen, facilitating the oxidative dehydrogenation of ammonia. The special electron interaction between ceria and tungsten oxides inhibited the reduction of Ce^{4+}. This effect is beneficial to form a WOx/CeO_2 structure bearing moderate oxidation ability. Ceria exhibits the worst activity and N_2 selectivity, due to its strongest abilities for ammonia and NO oxidation. For WOx/CeO_2 catalysts, the continuous decrease of reducibility caused by WOx modification restrains both NOx formation and ammonia oxidation. A similar mechanism exists in NO oxidation over all the tungsten-containing catalysts.

On the basis of the literature and our experiments, two tentative reaction routes for the SCR reaction over CeO_2 and WOx/CeO_2 catalysts are presented in Fig. 12. For ceria, a large amount of ammonia is mainly adsorbed on Lewis acid sites. The active surface oxygen accelerates the successive H-abstraction process of NH_3 to form NH_2 and NH species. NH then reacts with NO and O_2 to form N_2O and the further oxidation of NO generates NO_2 (Reactions (6)–(10)). The consumed surface oxygen can be rapidly supplemented by gaseous oxygen. For WOx-containing catalysts, the increased amount of acid sites due to tungsten modification promotes NH_3 adsorption. Meanwhile, the decreased amount of surface oxygen prevents the excessive de-protonation of NH_3 species to NH. More NH_2 species form from NH_3 deprotonated by bridging oxygen from W–O–Ce and W–O–W domains. NH_2 reacts with NO and O_2 to generate water and nitrogen. The decrease of surface oxygen inhibits the generation of NO_2 from NO. The oxygen vacancies left behind by the reaction of bridging oxygen are further oxidized by gaseous oxygen (Reaction (13)).

$$NH_3(ads) + O^* \longrightarrow NH_2(ads) + OH \quad (6)$$

$$NH_2(ads) + O^* \longrightarrow 2NH(ads) + OH \quad (7)$$

$$2NH(ads) + 2NO(gas) \rightarrow 2NHNO(ads) \longrightarrow N_2O + H_2O \quad (8)$$

$$NH(ads) + O^* \longrightarrow HNO(ads) \longrightarrow NO \quad (9)$$

$$NO(ads) + O^* \longrightarrow NO_2(ads) \rightarrow NO_2 \quad (10)$$

$$NH_2(ads) + NO\ (gas) \rightarrow NH_2NO(ads) \rightarrow N_2 + H_2O \quad (11)$$

$$2NH_2(ads) \rightarrow N_2H_4(ads) + O_2(gas) \rightarrow N_2 + 2H_2O \quad (12)$$

$$O_2 \longrightarrow 2O^* \quad (13)$$

"O*" represents surface active oxygen or bridging oxygen, "ads" represents adsorption species, and "gas" represents the gas phase species.

4 Conclusions

Both the acidity and redox properties of WOx/CeO_2 catalysts are determined by the structure of WOx species and the strong interaction between WOx and ceria, and thereby the activity and selectivity of WOx/CeO_2 catalysts is explained.

(1) 10WOx/CeO_2 calcined at 600°C shows the best SCR activity with a wide working temperature interval (NOx conversion > 80%) of 200–450°C.

(2) For all WOx/CeO_2 samples, isolated surface polytungstate is the main dominant species on ceria, and no crystalline WO_3 nanoparticles were observed. With increasing tungsten oxide loading, the electron interaction of WOx and CeO_2 increases, and the size of polytungstate domains grows.

(3) The modification by tungsten oxides also enhances the strength of the acid sites, which promotes the adsorption of ammonia and enhances the stability of adsorbed ammonia. The activity of surface oxygen is inhibited

with WOx loading, which is mainly caused by the strong interaction between WOx and CeO_2, leading to the lower oxidation ability of catalysts to inhibit NH_3 and NO oxidation, which favors the SCR reaction. These effects result in high NH_3-SCR activity and high selectivity for nitrogen with the tungsten containing catalysts.

Acknowledgments

The authors would like to acknowledge the Ministry of Science and Technology, PR China for financial support of Project 2010CB732304 and Science and Technology Department of Zhejiang Province Project 2011C31010. Moreover, we would also thank the State Key Lab of New Ceramics and Fine Process in Tsinghua University.

References

Adamowska M, Krzto A, Najbar M, Costa P D, Djéga-Mariadassou G, 2008. DRIFT study of the interaction of NO and O_2 with the surface of $Ce_{0.62}Zr_{0.38}O_2$ as deNOx catalyst. *Catalysis Today*, 137(2-4): 288–291.

Barton D G, Shtein M, Wilson R D, Soled S L, Iglesia E, 1999a. Structure and electronic properties of solid acids based on tungsten oxide nanostructures. *Journal of Physical Chemistry B*, 103(4): 630–640.

Barton D G, Soled S L, Meitzner G D, Fuentes G A, Iglesia E, 1999b. Structural and catalytic characterization of solid acids based on Zirconia modified by tungsten oxide. *Journal of Catalysis*, 181(1): 57–72.

Bigey C, Hilaire L, Maire G, 2001. WO_3CeO_2 and Pd/WO_3CeO_2 as potential catalysts for reforming applications: I. physicochemical characterization study. *Journal of Catalysis*, 198(2): 208–222.

Brandenberger S, Kröcher O, Tissler A, Althoff R, 2008. The state of the art in selective catalytic reduction of NOx by ammonia using metal-exchanged Zeolite catalysts. *Catalysis Reviews Science and Engineering*, 50(4): 492–531.

Busca G, Larrubia M A, Arrighi L, Ramis G, 2005. Catalytic abatement of NOx: Chemical and mechanistic aspects. *Catalysis Today*, 107-108: 139–148.

Busca G, Liett L, Ramis G, Berti F, 1998. Chemical and mechanistic aspects of the selective catalytic reduction of NOx by ammonia over oxide catalysts: A review. *Applied Catalysis B: Environmental*, 18(1-2): 1–36.

Casapu M, Kröcher O, Elsener M, 2009. Screening of doped MNOx-CeO_2 catalysts for low-temperature NO-SCR. *Applied Catalysis B: Environmental*, 88(3-4): 413–419.

Chen L, Li J H, Ge M F, Zhu R H, 2010. Enhanced activity of tungsten modified CeO_2/TiO_2 for selective catalytic reduction of NOx with ammonia. *Catalysis Today*, 153(3-4): 77–83.

Cormal A, Atienzar P, García H, Chane-Ching J, 2004. Hierarchically mesostructured doped CeO_2 with potential for solar-cell use. *Nature Material*, 3(6): 394–397.

Cortés-Jácome M A, Angeles-Chavez C, López-Salinas E, Navarrete J, Toribio P, Toledo J A, 2007. Migration and oxidation of tungsten species at the origin of acidity and catalytic activity on WO_3-ZrO_2 catalysts. *Applied Catalysis A: General*, 318: 178–189.

Dumesic J A, Topsøe N Y, Topsøe H, Chen Y, Slabiak T, 1996. Kinetics of selective catalytic reduction of nitric oxide by ammonia over Vanadia/Titania. *Journal of Catalysis*, 163(2): 409–417.

Gao X, Du X S, Cui L W, Fu Y C, Luo Z Y, Cen K F, 2010. A Ce-Cu-Ti oxide catalyst for the selective catalytic reduction of NO with NH_3. *Catalysis Communications*, 12(4): 255–258.

Gao X, Jiang Y, Zhong Y, Luo Z Y, Cen K F, 2010. The activity and characterization of CeO_2-TiO_2 catalysts prepared by the sol-gel method for selective catalytic reduction of NO with NH_3. *Journal of Hazardous Materials*, 174(1-3): 734–739.

Gregorio F D, Keller V, 2004. Activation and isomerization of hydrocarbons over WO_3/ZrO_2 catalysts I. Preparation, characterization, and X-ray photoelectron spectroscopy studies *Journal of Catalysis*, 225(1): 45–55.

Grossale A, Nova I, Tronconi E, 2008. Study of a Fezeolite-based system as NH_3-SCR catalyst for diesel exhaust after treatment. *Catalysis Today*, 136(1-2): 18–27.

Guisnet M, Magnoux P, 1997. Deactivation by coking of zeolite catalysts. Prevention of deactivation. Optimal conditions for regeneration. *Catalysis Today*, 36(4): 47–483.

Huang S J, Chen F C, Liu S L, Zhu Q J, Zhu X X, Xin W J et al., 2007. The influence of preparation procedures and tungsten loading on the metathesis activity of ethene and 2-butene over supported WO_3 catalysts. *Journal of Molecular Catalysis A: Chemical*, 267(1-2): 224–233.

Huang Y, Tong Z Q, Wu B, Zhang J F, 2008. Low temperature selective catalytic reduction of NO by ammonia over V_2O_5-CeO_2/TiO_2 *Journal of Fuel Chemistry and Technology*, 36(5): 616–620.

Kim T, Burrows A, Kiely C J, Wachs I E, 2007. Molecular/electronic structure-surface acidity relationships of model-supported tungsten oxide catalysts. *Journal of Catalysis*, 246(2): 370–381.

Klukowski D, Balle P, Geiger B, Wagloehner S, Kureti S, Kimmerle B et al., 2009. On the mechanism of the SCR reaction on Fe/HBEA zeolite. *Applied Catalysis B: Environmental*, 93(1-2): 185–193.

Li Y, Cheng H, Li D Y, Qin Y S, Xie Y M, Wang S D, 2008. WO_3/CeO_2-ZrO_2, a promising catalyst for selective catalytic reduction (SCR) of NOx with NH_3 in diesel exhaust. *Chemical Communications*, (12): 1470–1472.

Lin Q, Shimizu K, Satsuma A, 2009. Redox property of tungstated-zirconia analyzed by time resolved in situ UV-Vis spectroscopy. *Applied Catalysis A: General*, 365(1): 55–61.

Liu H D, Wei L Q, Yue R L, Chen Y F, 2010. CrO_x-CeO_2 binary oxide as a superior catalyst for NO reduction with NH_3 at low temperature in presence of CO. *Catalysis Communications*, 11(9): 829–833.

Liu Q Y, Liu Z Y, Li C Y, 2006. Adsorption and activation of NH_3 during selective catalytic reduction of NO by NH_3. *Chinese Journal of Catalysis*, 27(7): 636–646.

Mamede A S, Payen E, Grange P, Poncelet G, Ion A, Alifanti M et al., 2004. Characterization of WOx/CeO_2 catalysts and their reactivity in the isomerization of hexane. *Journal of Catalysis*, 223(1): 1–12.

Martin C, Malet P, Solana G, Rives V, 1998. Structural analysis of silica-supported tungstates. *Journal of Physical Chemistry B*, 102(15): 2759–2768.

Mineshige A, Taji T, Muroi Y, Kobune M, Fujii S, Nishi N et al., 2000. Oxygen chemical potential variation in ceria-based solid oxide fuel cells determined by Raman spectroscopy. *Solid State Ionics*, 135(1-4): 481–485.

Onfroy T, Clet G, Houalla M, 2005. Acidity, Surface Structure, and Catalytic Performance of WOx Supported on Monoclinic Zirconia. *Journal of Physical Chemistry B*, 109(8): 3345–3354.

Qi G, Yang R T, Chang R, 2004. MNOx-CeO_2 mixed oxides prepared by co-precipitation for selective catalytic reduction of NO with NH_3 at low temperatures. *Applied Catalysis B: Environmental* 51(2): 93–106.

Ramis G, Busca G, Bregani F, Forzatti P, 1990. Fourier transform-infrared study of the adsorption and coadsorption of nitric oxide, nitrogen dioxide and ammonia on vanadia-titania and mechanism of selective catalytic reduction. *Applied Catalysis*, 64: 259–278.

Ramis G, Yi L, Busca G, Turco M, Kotur E, Willey R J, 1995. Absorption, activation, and oxidation of ammonia over SCR catalysts. *Journal of Catalysis*, 157(2): 523–535.

Reddy B M, Khan A, Yamada Y, Kobayashi T, Loridant S, Volta J, 2002. Surface characterization of CeO_2/SiO_2 and $V_2O_5/CeO_2/SiO_2$ catalysts by Raman, XPS, and other techniques. *Journal of Physical Chemistry B*, 106(42): 10964–10972.

Reddy B M, Khan A, Yamada Y, Kobayashi T, Loridant S, Volta J, 2003. Structural characterization of CeO_2TiO_2 and V_2O_5/CeO_2TiO_2 catalysts by Raman and XPS techniques. *Journal of Physical Chemistry B*, 107(22): 5162–5176.

Santiesteban J G, Calabro D C, Borghard W S, Chang C D, Vartuli J C, Tsao Y P et al., 1999. H-spillover and SMSI effects in paraffin hydroisomerization over Pt/WOx/ZrO_2 Bifunctional Catalysts. *Journal of Catalysis*, 183(2): 314–322.

Schulz H, Stark W J, Maciejewski M, Pratsinis S E, Baiker A, 2003. Flame-made nanocrystalline ceria/zirconia doped with alumina or silica: structural properties and enhanced oxygen exchange capacity. *Journal of Materials Chemistry*, 13(12): 2979–2984.

Schwidder M, Heikens S, Toni A D, Geisler S, Berndt M, Brückner A et al., 2008. The role of NO_2 in the selective catalytic reduction of nitrogen oxides over Fe-ZSM-5 catalysts: Active sites for the conversion of NO and of NO/NO_2 mixtures. *Journal of Catalysis*, 259(1): 96–103.

Shan W P, Liu F D, He H, Shi X Y, Zhang C B, 2011. Novel cerium-tungsten mixed oxide catalyst for the selective catalytic reduction of NOx with NH_3. *Chemical Communications*, 47(28): 8046–8048.

Si Z C, Weng D, Wu X D, Jiang Y, 2010. Roles of Lewis and Brönsted acid sites in NO reduction with ammonia on CeO_2-ZrO_2-NiO-SO_4^{2-} catalyst. *Journal of Rare Earths*, 28(5): 727–731.

Singh G P, Singh D P, 2011. Effect of WO_3 on structural and optical properties of CeO_2-PbO-B_2O_3 glasses. *Physica B: Condensed Matte*, 406(3): 640–644.

Sjövall H, Blint R J, Olsson L, 2009. Detailed kinetic modeling of NH_3 SCR over Cu-ZSM-5. *Applied Catalysis B: Environmental*, 92(1-2): 138–153.

Tsunekawa S, Fukuda T, Kasuya A, 2000. Blue shift in ultraviolet absorption spectra of monodisperse CeO_{2x} nanoparticles. *Journal of Applied Physics*, 87(3): 1318–1321.

Vargas M A L, Casanova M, Trovarelli A, Busca G, 2007. An IR study of thermally stable V_2O_5-WO_3-TiO_2 SCR catalysts modified with silica and rare-earths (Ce, Tb, Er). *Applied Catalysis B: Environmental*, 75(3-4): 303–311.

Vidal H, Kašpar J, Pijolat M, Colon G, Bernal S, Cordón A et al., 2000. Redox behavior of CeO_2ZrO_2 mixed oxides I. Influence of redox treatments on high surface area catalysts. *Applied Catalysis B: Environmental*, 27(1): 49–63.

Wachs I E, Kim T, Ross E I, 2006. Catalysis science of the solid acidity of model supported tungsten oxide catalysts. *Catalysis Today*, 116(2): 162–168.

Wang X H, Lu G Z, Guo Y, Xue Y Y, Jiang L Z, Guo Y L et al., 2007. Structure, thermal-stability and reducibility of Si-doped Ce-Zr-O solid solution. *Catalysis Today*, 126(3-4): 412–419.

Xu W D, He H, Yu Y B, 2009. Deactivation of a Ce/TiO_2 catalyst by SO_2 in the selective catalytic reduction of NO by NH_3. *Journal of Physical Chemistry C*, 113(11): 4426–4432.

Yagoubi B, Hogarth C A, 1993. Effect of cerium oxide addition on the optical absorption edge of tungsten trioxide. *Journal of Materials Science*, 28(1): 239–242.

Zhu J, Gao F, Dong L H, Yu W J, Qi L, Wang Z et al., 2010. Studies on surface structure of $M_xO_y/MoO_3/CeO_2$ system (M=Ni, Cu, Fe) and its influence on SCR of NO by NH_3. *Applied Catalysis B: Environmental*, 95(1-2): 144–152.

JOURNAL OF ENVIRONMENTAL SCIENCES

Journal of Environmental Sciences (Established in 1989)
Vol. 24 No. 7 2012

Supervised by	Chinese Academy of Sciences	**Published by**	Science Press, Beijing, China
Sponsored by	Research Center for Eco-Environmental		Elsevier Limited, The Netherlands
	Sciences, Chinese Academy of Sciences	**Distributed by**	
Edited by	Editorial Office of Journal of	Domestic	Science Press, 16 Donghuangchenggen
	Environmental Sciences (JES)		North Street, Beijing 100717, China
	P. O. Box 2871, Beijing 100085, China		Local Post Offices through China
	Tel: 86-10-62920553; http://www.jesc.ac.cn	Foreign	Elsevier Limited
	E-mail: jesc@263.net, jesc@rcees.ac.cn		http://www.elsevier.com/locate/jes
Editor-in-chief	Hongxiao Tang	**Printed by**	Beijing Beilin Printing House, 100083, China

CN 11-2629/X **Domestic postcode: 2-580** **Domestic price per issue RMB ¥ 110.00**

ISSN 1001-0742